Supporting Information

Template-Free Synthesis of Uniform Magnetic Mesoporous TiO_2 Nanospindles for Highly Selective Enrichment of Phosphopeptides

Wei Li,[†] Minbo Liu,[‡] Shanshan Feng,[†] Xiaomin Li,[†] Jinxiu Wang,[†] Dengke Shen,[†] Yuhui Li,[†] Zhenkun Sun,[†] Ahmed A. Elzatahry,[§,#] Haojie Lu,[,‡] and Dongyuan Zhao*[,†]*

† Department of Chemistry, Laboratory of Advanced Materials, Shanghai Key Lab of Molecular Catalysis and Innovative Materials, and State key Laboratory of Molecular Engineering of Polymers, Fudan University, Shanghai 200433, P. R. China.

‡ Department of Chemistry and Institutes of Biomedical Sciences,Fudan University, Shanghai 200032, P. R. China.

§ Department of Chemistry-College of Science, King Saud University, Riyadh 11451, Saudi Arabia.

Polymer Materials Research Department, Advanced Technology and New Materials Research Institute, City of Scientific Research and Technology Applications, New Borg El-Arab City, Alexandria 21934, Egypt.

Email: dyzhao@fudan.edu.cn, luhaojie@fudan.edu.cn

Experimental Section

Materials. $FeCl_3 \cdot 6H_2O$, potassium dihydrogen phosphate (KH_2PO_4), tetrabutyl titanate (TBOT), ethanol and concentrated ammonia solution (28 wt%) were of analytical grade and purchased from Shanghai Chemical Corp. β-casein (bovine, 99%), bovine serum albumin (BSA, 95%), ammonium bicarbonate and 2,5-dihydroxybenzoic acid (2,5-DHB, 98%) were purchased from Sigma (St. Louis, MO). All chemicals were used as received without further purification. Deionized water was used for all experiments.

Preparation of α-Fe_2O_3 nanospindles. The α-Fe_2O_3 nanospindles were prepared by aging a solution of $FeCl_3$ (0.02 M) and KH_2PO_4 (0.45 mM) at 105 °C for 48 h. The obtained products were separated and collected by centrifugation, followed by washing with deionized water and ethanol for 3 times, respectively.

Preparation of α-Fe_2O_3@TiO_2 and α-Fe_2O_3@TiO_2-500 samples. α-Fe_2O_3@TiO_2 core-shell nanospindles were prepared in the facile Stöber system. The α-Fe_2O_3 nanospindles were dispersed in absolute ethanol (100 mL), and mixed with concentrated ammonia solution (0.40 mL, 28 wt%) under ultrasound for 15 min. Afterward, 0.75 mL of TBOT was added dropwise in 5 min, and the reaction was allowed to proceed for 24 h at 45 °C under continuous mechanical stirring. The resultant products were separated and collected by centrifugation, followed by washing with ethanol. The final samples (denoted as α-Fe_2O_3@TiO_2) were dried at 60 °C. After calcination at 500 °C in air for 2 h, the α-Fe_2O_3@TiO_2-500 samples were obtained.

Preparation of uniform mesoporous α-Fe_2O_3@mTiO_2 and α-Fe_2O_3@mTiO_2-500 nanospindles. The uniform mesoporous α-Fe_2O_3@mTiO_2 core-shell nanospindles were prepared based on a new "post-hydrolysis" concept. The resultant α-Fe_2O_3@TiO_2 samples before calcination were subjected to an additional ultrasonic treatment in water. In a typical process, the as-made α-Fe_2O_3@TiO_2 samples were immersed into a glass bottle with 20 mL water, and then placed in a continuous ultrasound bath (DL-180A, 180W, Shanghai Zhisun Instrument Co., Ltd.) for 6 h. During the ultrasound process, the bath temperature was held at 20 °C by the refluxing water. The final samples (denoted as α-Fe_2O_3@mTiO_2) were separated and collected by centrifugation, followed by washing with ethanol and dried at 60 °C. After calcination at 500 °C in air for 2 h, the mesoporous α-Fe_2O_3@mTiO_2-500 samples were obtained.

Preparation of uniform magnetic mesoporous Fe_3O_4@mTiO_2 nanospindles. Uniform magnetic mesoporous Fe_3O_4@mTiO_2 core-shell nanospindles were simply obtained by reducing the α-Fe_2O_3@mTiO_2-500 nanospindles at 400 °C under a continuous H_2/Ar gas flow (5 % H_2) for 4 h. Then the furnace was allowed to cool to room temperature while still under a continuous H_2/Ar gas flow.

Tryptic digestion of standard proteins. Each protein, β-casein or BSA, was first dissolved in ammonium bicarbonate (25 mM, pH 8.0) and then denatured by boiling for 10 min. Trypsin was added into the solution at an enzyme/substrate ratio of 1:40 (w/w) and incubated at 37 °C for 12 h.

Selective enrichment of phosphopeptides. The phosphopeptide enrichment is performed with the Fe_3O_4@mTiO_2 and Fe_3O_4@TiO_2 samples, respectively. The resultant products were washed by ethanol for three times and then dispersed in deionized water, respectively (10 $mgmL^{-1}$). For each experiment 2 μL of products was incubated with 100 μL of loading buffer (0.1% TFA, 50% acetonitrile) and peptide mixture for 60 min at room temperature. After separated by applying an external magnetic field, the nanoparticles with captured phosphopeptides were washed with loading buffer for three times. For elution of bound phosphopeptides, the material was incubated with 10 μL of 5% $NH_3 \cdot H_2O$, and the phosphopeptides were collected for further MS analysis.

MALDI Mass Spectrometry. MALDI MS analysis was performed an Applied Biosystems 5800 Proteomics Analyzer. The sample solution (0.5 μL) was spotted onto a MALDI target and then air-dried, followed by addition of 0.5 μL of DHB matrix solution (0.1% TFA, 50% acetonitrile). Positive ion reflector mode was performed, and the spectrum of each spot was obtained by accumulation of 2000 laser shots.

Characterizations. Wide-angle XRD patterns were recorded on a Bruker D8 diffractometer (Germany) with Ni-filtered Cu Kα radiation (40 kV, 40 mA). Nitrogen sorption isotherms were measured at 77 K with a Micromeritcs Tristar 3020 analyzer. All of the samples were degassed under vacuum at 180 °C for at least 8 h prior to measurement. The Brunauer-Emmett-Teller (BET) method was utilized to calculate the specific surface areas using adsorption data in a relative pressure range from 0.05

to 0.25. The pore size distributions (PSD) were derived from the adsorption branch of the isotherms using the Barrett-Joyner-Halenda (BJH) model. The total pore volume V_t was estimated from the adsorbed amount at a relative pressure P/P_0 of 0.995. Transmission electron microscopy (TEM) experiments were conducted on a JEOL JEM-2100 F microscope (Japan) operated at 200 kV. The samples for the TEM measurements were suspended in ethanol and supported onto a holey carbon film on a Cu grid. Field-emission scanning electron microscopy (FESEM) images were taken on a Hitachi S-4800 microscope. Fourier transform infrared (FTIR) spectra were recorded on a Nicolet Nexus 470 spectrometer using spectroscopic grade KBr. X-ray photoelectron spectroscopy (XPS) experiments were carried out on a RBD upgraded PHI-5000C ESCA system (Perkin Elmer) with Mg Ka radiation (hv = 1253.6 eV). Magnetic characterization was carried out with a vibrating sample magnetometer on a Model 6000 Physical Property Measurement System (Quantum, USA) at 300 K.

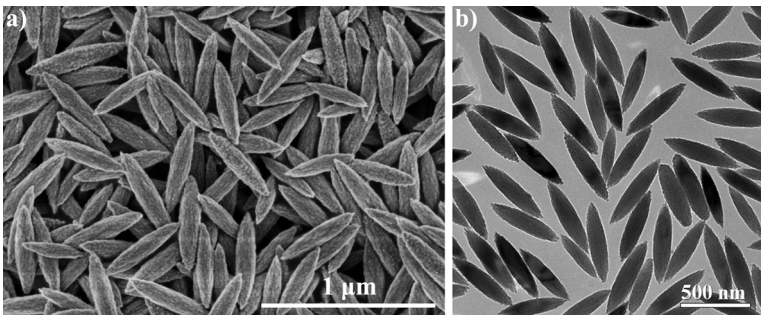

Figure S1. FESEM and TEM images of the α-Fe_2O_3 nanospindles prepared by aging a solution of $FeCl_3$ (0.02 M) and KH_2PO_4 (0.45 mM) at 105 °C for 48 h.

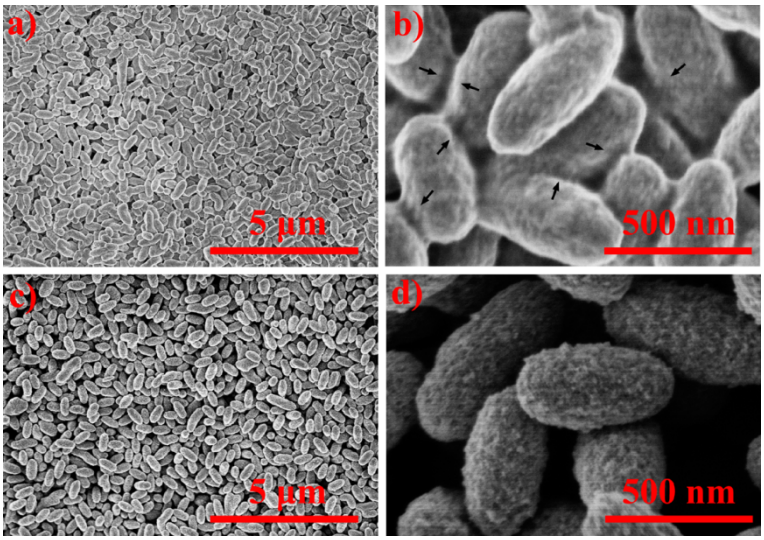

Figure S2. FESEM images of (a,b) the α-Fe_2O_3@TiO_2 core-shell nanospindles and (c,d) the uniform mesoporous α-Fe_2O_3@mTiO_2 core-shell nanospindles. The arrows clearly indicate the linkages between the α-Fe_2O_3@TiO_2 core-shell nanospindles.

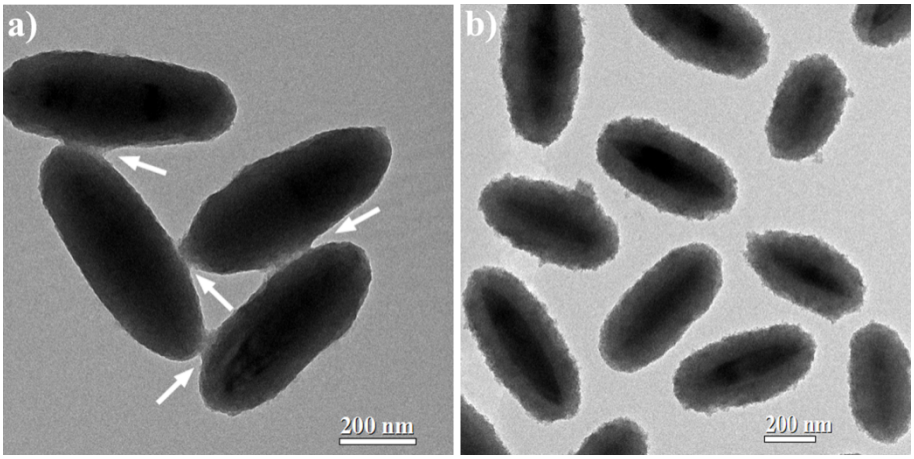

Figure S3. TEM images of (a) the α-Fe_2O_3@TiO_2 core-shell nanospindles and (b) the uniform mesoporous α-Fe_2O_3@mTiO_2 core-shell nanospindles. The arrows clearly disclose the linkages between the α-Fe_2O_3@TiO_2 core-shell nanospindles.

Table S1. Textual and adsorption properties of the resultant core-shell nanospindles.

Sample	BET surface area (m^2/g)	Pore size (nm)	Enrichment capacity (mg/g)*
α-Fe_2O_3@TiO_2	119	< 1.7	
α-Fe_2O_3@mTiO_2	366	2.6	
α-Fe_2O_3@TiO_2-500	21	7.3	75
α-Fe_2O_3@mTiO_2-500	117	5.4	300

* The enrichment capacity of phosphopeptides with the magnetic derivative products.

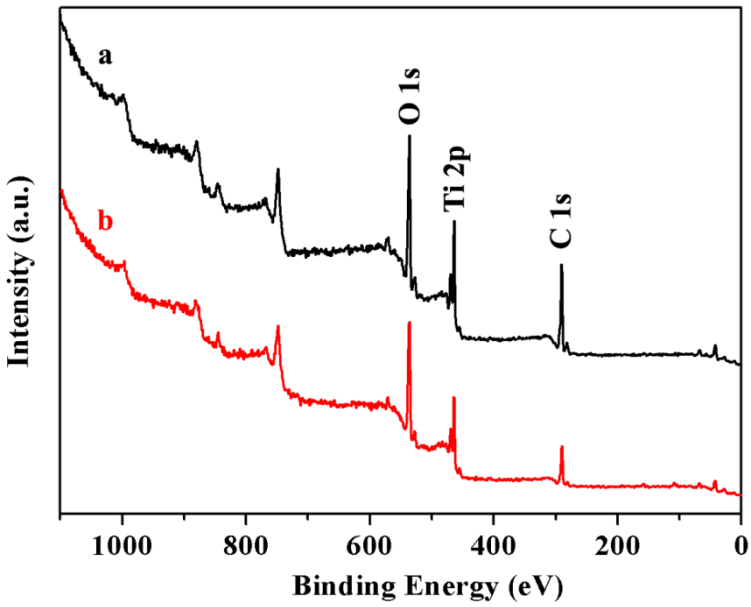

Figure S4. XPS spectra of (a) the α-Fe_2O_3@TiO_2 core-shell nanospindles and (b) the uniform mesoporous α-Fe_2O_3@mTiO_2 core-shell nanospindles.

Table S2. Contents of C, O, Ti and different oxygen species in the surface of α-Fe_2O_3@TiO_2 and α-Fe_2O_3@mTiO_2 core-shell nanospindles.

Samples	C (%)	O (%)	Ti (%)	O 1s		
				Ti–O (%)	C–O (%)	O–H (%)
α-Fe_2O_3@TiO_2	52.9	37.1	10.0	50.2	22.9	26.9
α-Fe_2O_3@mTiO_2	38.9	48.2	12.9	49.5	11.5	39.0

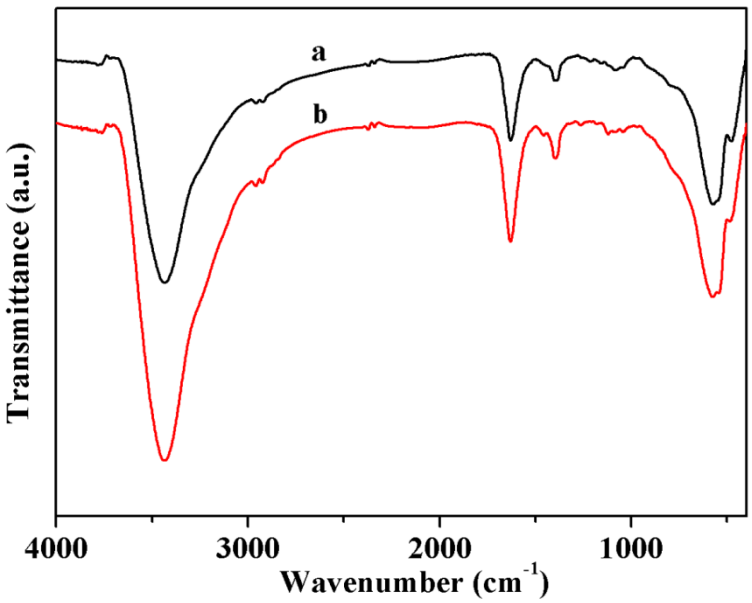

Figure S5. FTIR spectra of (a) the α-Fe_2O_3@TiO_2 core-shell nanospindles and (b) the uniform mesoporous α-Fe_2O_3@mTiO_2 core-shell nanospindles.

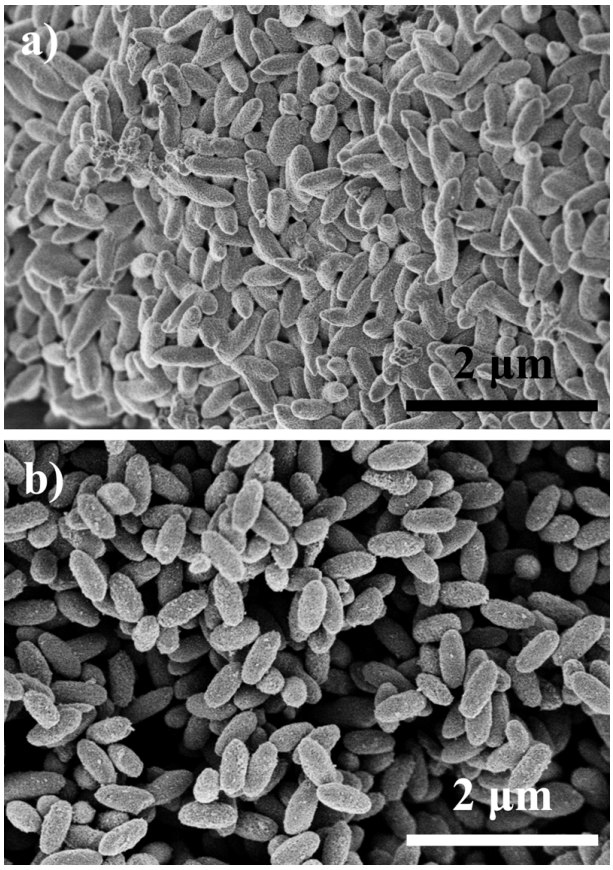

Figure S6. FESEM image of the α-Fe_2O_3@TiO_2-500 (a) and α-Fe_2O_3@mTiO_2-500 (b) samples, respectively.

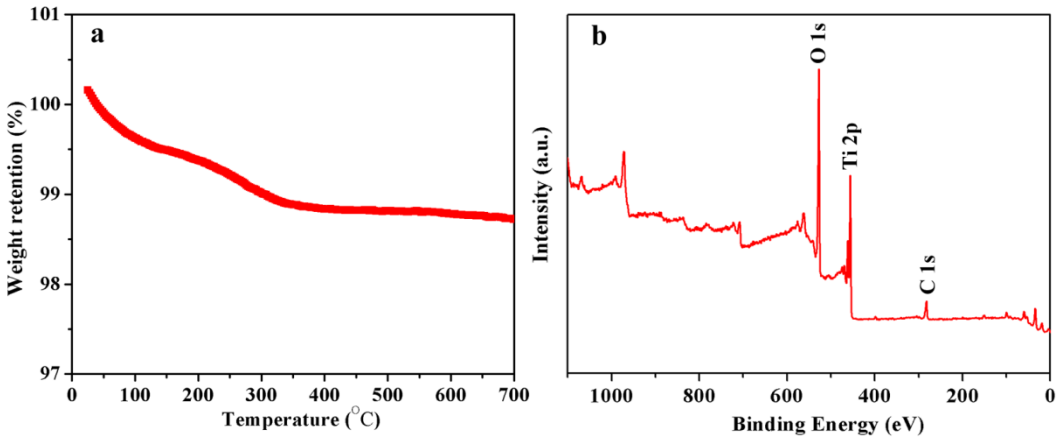

Figure S7. (a) A typical TGA curve obtained for the mesoporous α-Fe_2O_3@mTiO_2-500 nanospindles under O_2. Approximately 0.5 % weight loss was observed at a temperature around 200 – 450 °C. (b) The XPS spectrum of the mesoporous α-Fe_2O_3@mTiO_2-500 nanospindles.

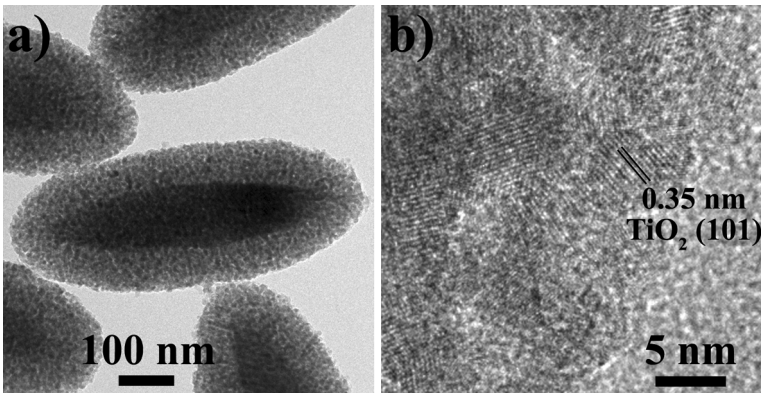

Figure S8. TEM (a) and HRTEM (b) images of the uniform mesoporous α-Fe_2O_3@mTiO_2-500 core-shell nanospindles.

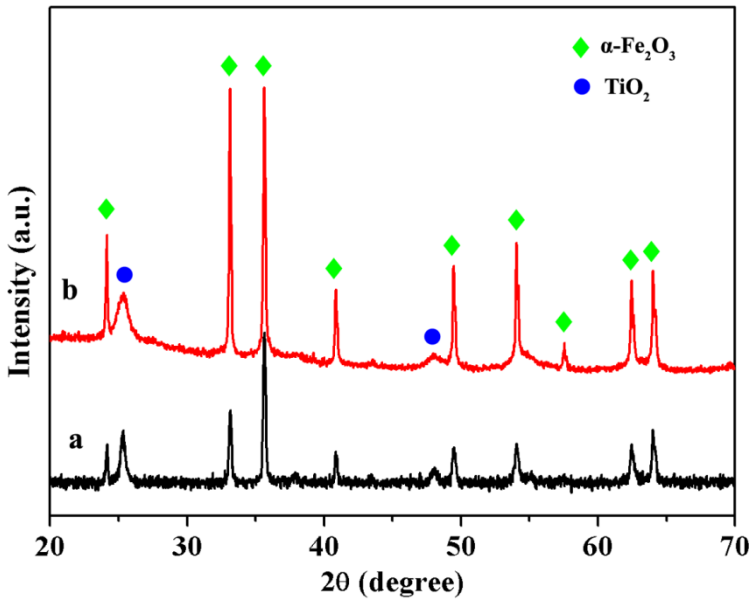

Figure S9. XRD patterns of the α-Fe_2O_3@TiO_2-500 (a) and α-Fe_2O_3@mTiO_2-500 (b) samples, respectively. The blue spheres (●) and green rhombuses (◆) indicate the typical diffraction peaks of anatase TiO_2 and α-Fe_2O_3, respectively.

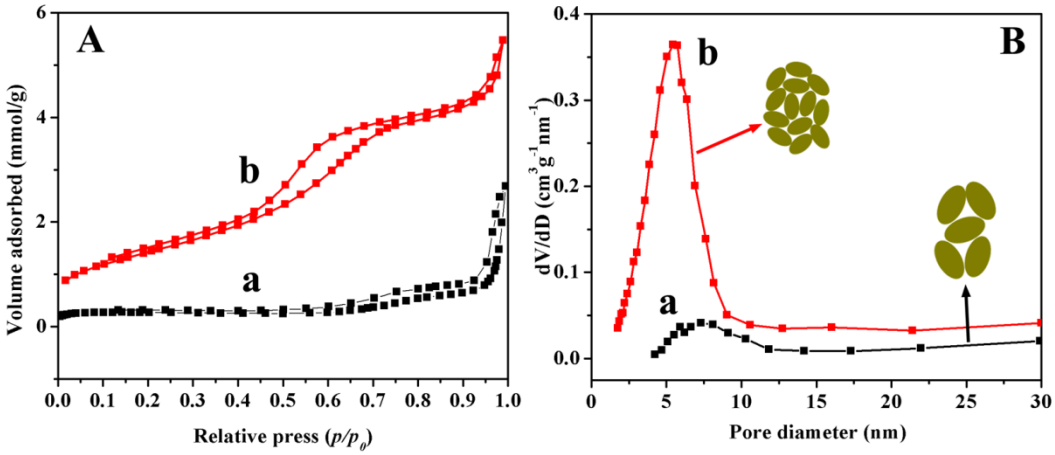

Figure S10. N_2 sorption isotherms (A) and the corresponding pore size distribution curves (B) of the α-Fe_2O_3@TiO_2-500 (a) and α-Fe_2O_3@mTiO_2-500 (b) samples, respectively. The insets in B are the corresponding schematic illustrations of the porous structures.

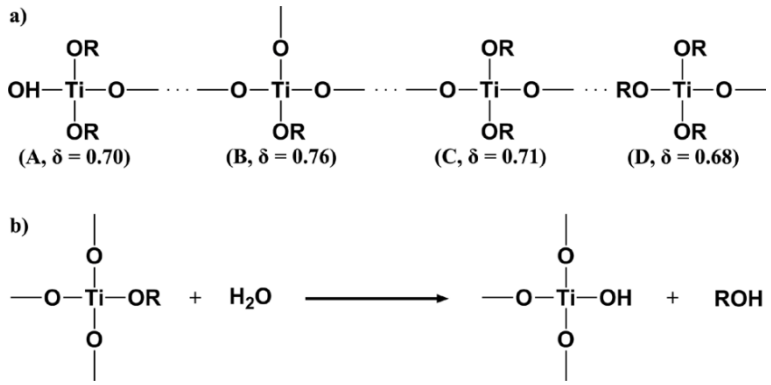

Figure S11. (a) The typical partially hydrolyzed polymers during the hydrolysis and condensation of titanium alkoxides. The values of δ (Ti) for sites A-D are calculated from the partial-charge model. Since the values are presented as B >> C ≈ A > D, the order reactivity of the partially hydrolyzed polymers toward nucleophilic attack should decrease as B >> C ≈ A > D. Thus, the middle structures rather than the ends of completely cross-linked chains are perfectly obtained, which leads to the resultant compact and highly branched polymer matrix. (b) The typical reaction during the post-hydrolysis process.

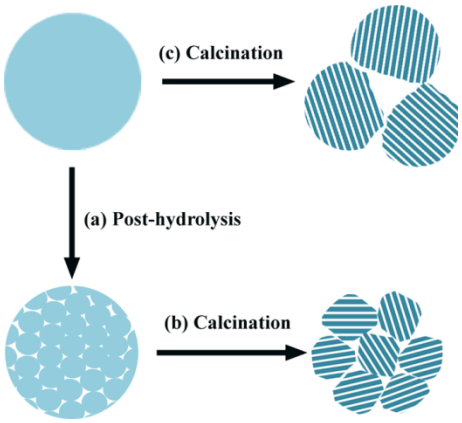

Figure S12. The schematic illustratation of the structure evolution of the TiO_2 shell during the additional post-hydrolysis and annealing process.

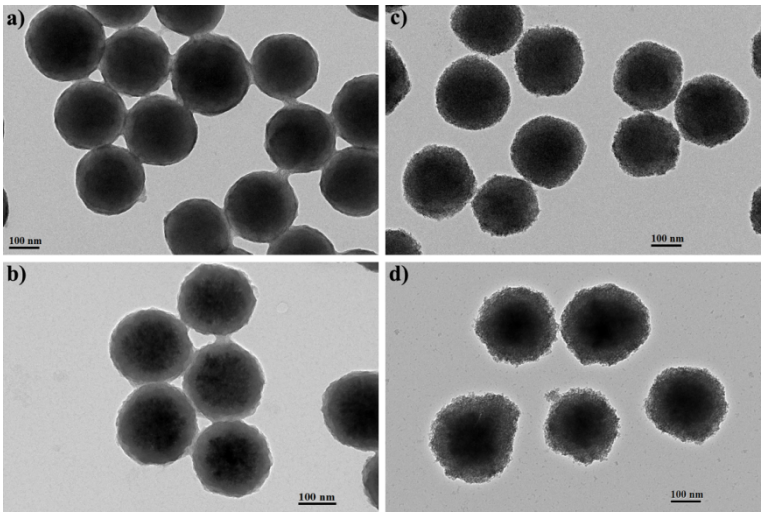

Figure S13. TEM images of (a, c) the SiO_2@mTiO_2 and (b, d) the Fe_3O_4@mTiO_2 core-shell nanoparticles before and after the post-hydrolysis process. Fe_3O_4 nanoparticles were prepared by aging a solution of $FeCl_3 \cdot 6H_2O$ (3.25 g), trisodium citrate (1.3 g), and sodium acetate (NaAc, 6.0 g) and ethylene glycol (100 mL) at 200 °C for 10 h. SiO_2 spheres were prepared in a typical sol-gel coating process. TEOS (3.8 mL), concentrated ammonia solution (28 wt%, 7.5 mL) and deionized water (18 mL) were mixed into ethanol (120 mL), and stirred at 25 °C for 24 h.

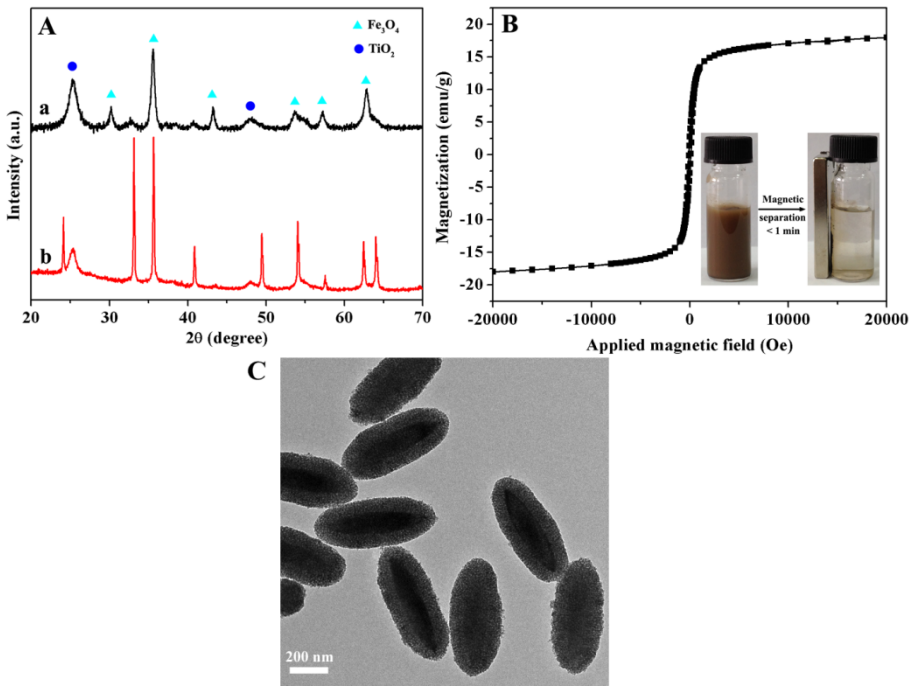

Figure S14. XRD patterns (A) of the uniform magnetic mesoporous Fe_3O_4@mTiO_2 (a) and α-Fe_2O_3@mTiO_2-500 (b) core-shell nanospindles. The spheres (●) and triangles (▲) indicate the typical diffraction peaks of anatase TiO_2 and Fe_3O_4, respectively. (B) The magnetic hysteresis loops at 300 K of the uniform magnetic mesoporous Fe_3O_4@mTiO_2 nanospindles. The inset in B clearly shows that the uniform magnetic mesoporous Fe_3O_4@mTiO_2 nanospindles can be conveniently separated upon application of an external magnetic field. (C) TEM image of the uniform magnetic mesoporous Fe_3O_4@mTiO_2 core-shell nanospindles.

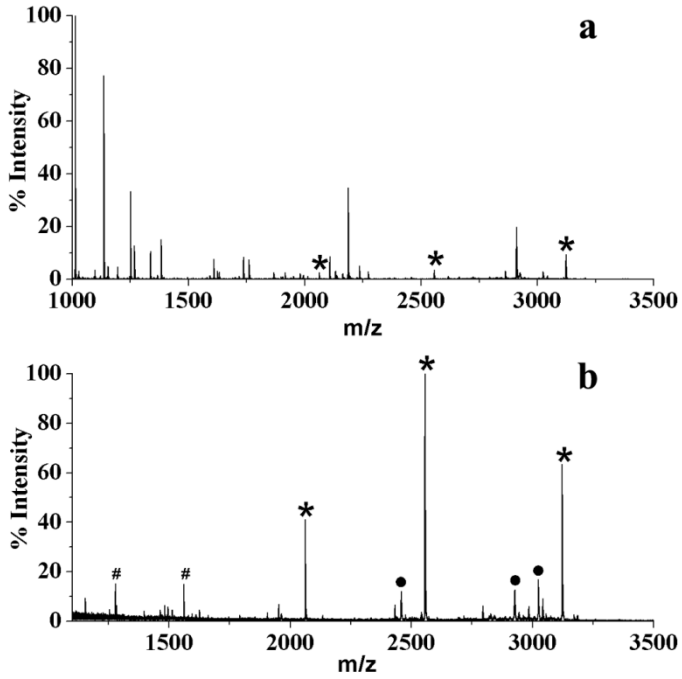

Figure S15. MALDI mass spectra of tryptic digest of standard protein β-casein before (a) and after (b) enrichment with the uniform magnetic mesoporous Fe_3O_4@mTiO_2 nanospindles. The asterisks indicate the phosphopeptides, the circles indicate the dephosphorylated counterparts, and the pounds indicate the phosphopeptides with doubly charged.